

# Development of Gastroretentive Floating Pellets to Enhance the Oral Bioavailability of Lurasidone Hydrochloride

A JOSHI\* AND A GORLE

R. C. Patel Institute of Pharmaceutical Education and Research, Shirpur, Dhule, North Maharashtra University, Jalgaon, India

## Joshi *et al.*: Gastroretentive Floating Pellets

Lurasidone hydrochloride exhibits pH-sensitive solubility, which limits its absorption and results in poor oral bioavailability. To address this problem, the present study focused on the formulation of gastro retentive floating pellets of lurasidone hydrochloride using the extrusion-speronization technique to enhance gastric retention, solubility, and plasma concentration. The 33 Box-Behnken design was applied to optimize the formulation batch. For that, the levels of HPMC K100 (X1), ethyl cellulose (X2), and spheronization speed (X3) were varied, and their influence was evaluated on aspect ratio (Y1), floating time (Y2), and *in vitro* % drug release (Y3). The observed optimized batch was subsequently coated with a 5 % ethyl cellulose and subjected to a comprehensive physicochemical evaluation with % drug release and *in vivo* pharmacokinetic assessment. The drug release data observed that the coated lurasidone hydrochloride pellets release the drug over 18 h, whereas the uncoated pellets release up to 12 h. The ethyl cellulose coating also improved the buoyancy, which minimizes dose dumping and improves the absorption window of lurasidone hydrochloride in the upper GI tract. The relative oral bioavailability of uncoated and coated pellets was significantly higher, up to 5-fold and 7-fold, respectively, compared to pure lurasidone hydrochloride. It strongly supports the hypothesis that coated lurasidone hydrochloride gastro retentive floating pellets could enhance oral bioavailability instead of pure lurasidone hydrochloride.

**Key words:** Lurasidone hydrochloride, spheronization, gastro retentive pellets, buoyancy, oral bioavailability

In the domain of pharmaceutical sciences, more than one-third of therapeutic agents fall under the Biopharmaceutical Classification System (BCS) class II, belonging to high permeability but low water solubility. Their limited solubility often restricts dissolution in the gastrointestinal tract, leading to suboptimal oral bioavailability. Consequently, there is a need to design an advanced drug delivery system to overcome these solubility-driven limitations.

Lurasidone Hydrochloride (LSH) is one of them that possesses potential efficacy to treat a number of psychotic conditions<sup>[1,2]</sup>. Commercially, it is available in a conventional tablet with the brand name Latuda®, but it suffers from pH-dependent solubility and slow dissolution. It preferentially uptakes from the proximal gastrointestinal tract at pH<sup>[3,4]</sup>. Therefore, it is associated with a narrow absorption window and possesses only 19 % oral bioavailability.

Furthermore, its short elimination half-life makes a dose optimization challenge and complicates its effective systemic delivery<sup>[3]</sup>. Therefore, its absorption has been affected by gastrointestinal transit time, and it is difficult to formulate an extended-release dosage form<sup>[4]</sup>. Thus, it becomes essential to alter the release profile of LSH, enabling sustained delivery over an extended period while simultaneously improving its dissolution rate. The suitable strategy to accomplish this is a Gastro Retentive Drug Delivery System (GRDDS). Among various GRDDS, Floating Drug Delivery Systems (FDDES) represent a significant advancement, particularly for those that are

This is an open access article distributed under the terms of the Creative Commons Attribution-NonCommercial-ShareAlike 3.0 License, which allows others to remix, tweak, and build upon the work non-commercially, as long as the author is credited and the new creations are licensed under the identical terms

Accepted 25 February 2026

Revised 22 January 2026

Received 13 December 2025

Indian J Pharm Sci 2026;88(1):21-37

\*Address for correspondence

E-mail: joshiakash202@outlook.com

predominantly absorbed from the proximal GI tract. As FDDS helps to extend the gastric retention and reduce gastrointestinal transit, it becomes supportive in enhancing the absorption window of LSH<sup>[5,6]</sup>.

This innovation offers several clinical advantages, including a steady and controlled release of medication. It also supports prolonging the drug action with brief half-lives, improving drug bioavailability, minimizing adverse effects, decreasing the frequency of doses, and augmenting the solubility of drugs that are less soluble in environments with elevated pH levels<sup>[7,8]</sup>. Thereby increasing the Gastric Retention Time (GRT), it stabilizes drug levels in the plasma. Further, it will be expelled from the stomach<sup>[6]</sup>. Nevertheless, the efficacy of these formulations is frequently compromised by obstacles related to adequate drug absorption, which are influenced by physiological variances in the gastrointestinal transit times and the gastric retention duration of these dosage forms<sup>[9]</sup>.

Therefore, the present study focused on multi-particulate drug delivery systems that include thousands of minuscule spherical particles, also known as pellets, each measuring between 0.05 to 2.00 mm in diameter. In this system, the active ingredient was distributed across numerous small units, which may be encased in capsules, enveloped in a pouch, or compressed into tablets to deliver the required dosage. The diminutive size of these particles presents several advantages over monolithic systems, including a reduced dependency on gastric emptying rates, thus mitigating variability in gastrointestinal transit times both within and between individuals. This formulation is pursued for its potential to enhance bioavailability by minimizing dosing frequency and gastric irritation<sup>[10]</sup>.

As a result, LSH was formulated into gastro retentive floating pellets using the extrusion-spheronization technique, with optimization of the concentrations

of HPMC K100, ethyl cellulose, and spheronizing speed. The formulated gastro retentive floating pellets ensure the expedited release of LSH within the gastric environment and increase oral bioavailability.

## MATERIALS AND METHODS

LSH was acquired from Emcure Pharmaceuticals. The HPMC K100 and ethyl cellulose were procured through Colorcon Asia Pvt. Ltd., India. While Microcrystalline Cellulose (MCC) was procured from JRS Pharma, Mumbai, India. Additionally, sodium bicarbonate was available from Merck Specialities Private Limited. The components, PVP K30 and magnesium stearate, were supplied by Zim Labs in Nagpur, India, and other important excipients were procured from Loba Chemie Pvt. Ltd., Mumbai, India.

### Experimental design:

The formulation of gastro retentive floating pellets incorporating LSH was executed utilizing the extrusion-spheronization technique, with subsequent drying conducted in a fluidized bed dryer (VJ instrument, spray nozzle 1.00mm, Tech Innovations, India).

The three factors in a three-level Box-Behnken experimental design were systematically adopted to optimize the LSH pellet formulation. The independent factors incorporated into this design included HPMC K 100 M concentration (X1), ethyl cellulose concentration (X2), and spheronization speed (X3) as depicted in Table 1. The corresponding dependent variables were selected, including the aspect ratio (Y1), total floating time (Y2), and % drug release, which collectively served as critical formulation responses<sup>[11,12]</sup>. The methodology comprised conducting 13 experimental trials, employing Analysis Of Variance (ANOVA), and undertaking optimization employing Design-Expert software, version 13.

**TABLE 1: EXPERIMENTAL FACTORS FOR THE FORMULATION AND OPTIMIZATION OF GASTRO-RETENTIVE FLOATING PELLETS (FOR 100 mg TOTAL TABLET WEIGHT)**

In dependable variables	Variable levels	Family	Family
	Low (-1)	Medium (0)	High (+1)
Concentration of HPMC K100 (%)	15	17.5	20
Concentration of ethyl cellulose (%)	15	17.5	20
Spheronizing speed (RPM)	750	800	850

### Preparation of LSH Gastro Retentive Floating Pellets (LSH-GRFP):

The formulation batches process began with LSH (8 % w/w) and excipients listed in Table 2 by following the Box-Behnken experimental design. All components were precisely weighed and then passed through a sieve number 40. These components were uniformly mixed in a conical blender for 10 min. Water was gradually added to the blend until the formation of a cohesive mass<sup>[13]</sup>.

This dough mass underwent extrusion using a mini screw extruder equipped with a 1 mm pore size, operating at variable speeds between 20 and 40 rpm. The extrudates produced were collected and then spheronized (VJ instrument, Tech Innovations, India) at speeds of 750, 800, and 850 rpm for 15 min, as represented in Table 2. Then, drying of the core pellets was carried out using a fluidised bed dryer at 70° for 10 min to achieve adequate moisture removal<sup>[14]</sup>.

**TABLE 2: FORMULATION BATCHES OF GASTRORETENTIVE FLOATING PELLETS OF LSH (500 mg TOTAL TABLET WEIGHT)**

Ingredient	Batches (Quantity in mg)												
	FP1	FP2	FP3	FP4	FP5	FP6	FP7	FP8	FP9	FP10	FP11	FP12	FP13
Lurasidone	40	40	40	40	40	40	40	40	40	40	40	40	40
HPMC K 100	75	100	100	87.5	87.5	75	87.5	87.5	75	100	100	75	87.5
Ethyl cellulose	75	87.5	87.5	75	100	87.5	100	87.5	100	75	100	87.5	75
Microcrystalline cellulose	220	182.5	182.5	207.5	182.5	207.5	182.5	195	195	195	170	207.5	207.5
Sod.Bicarbonate	60	60	60	60	60	60	60	60	60	60	60	60	60
PVP K 30	10	10	10	10	10	10	10	10	10	10	10	10	10
Magnesium Stearate	10	10	10	10	10	10	10	10	10	10	10	10	10
Talc	10	10	10	10	10	10	10	10	10	10	10	10	10
Water	Q.S	Q.S	Q.S	Q.S	Q.S	Q.S	Q.S	Q.S	Q.S	Q.S	Q.S	Q.S	Q.S
Total	500	500	500	500	500	500	500	500	500	500	500	500	500
Speronizing speed (RPM)	800	850	750	750	850	850	750	800	800	800	800	750	850

### Coating of LSH-GRFP:

The optimised batch of LSH-GRFP was further coated with ethyl cellulose using a fluidized bed dryer to extend the drug release. The 5 % w/w ethyl cellulose was ready by dissolving the polymer in isopropyl alcohol and stirring until a clear homogeneous solution was obtained. For the coating process, a 10 g batch of LSH optimised pellets was inserted in a basket of a fluidized bed dryer, with inlet and product temperatures maintained at 40° and 35°, respectively. During coating, the air flow was regulated between 0.7-0.9 bar, and the spray pressure was kept within 0.6-0.8 bar, respectively. The spraying rate was followed by 0.132 g/min to achieve 5 % w/w weight

gain. Following, the pellets were subjected to final drying at 40° for 15 min<sup>[15]</sup>.

### The drug content:

The Shu-sun *et al.* stated procedure was employed to quantify the drug content from both uncoated and coated pellets. For the preparation of the standard solution, precisely weighed 40 mg of pure LSH and dissolved in 10 ml of 0.1 N HCL. Similarly, the test solution was prepared by triturating an equivalent amount of 40 mg of LSH from LSH-GRFP (coated and uncoated) and also dispersed in 10 ml of 0.1 N HCL. The absorbance of both samples was measured at 227 nm using a Ultra Violet (UV)-visible

spectrophotometer (UV-1800, Shimadzu, Japan). Followed by the obtained absorbance was added to the linearity equation of LSH, and determined its concentration was determined. These concentrations were added in Equation 1 to obtain drug content<sup>[16]</sup>.

Drug content (%)=(Concentration of LSH detected in the test sample)/(The concentration of LSH detected in the standard sample)×100 (1)

#### **Micromeritic properties:**

The flow property of both uncoated and coated LSH-GRFP was assessed by determining different micromeritics properties, including Carr's index, Hausner's ratio, and angle of repose. The analysis of particle size distribution for the pellets was conducted through sieve analysis utilizing sieves numbered 20, 22, 30, 44, and 60. The sieves of the mechanical shaker were systematically organized in descending order and subjected to shaking for a duration of 15-20 min. The pellets retained on each sieve were collected, weighed, and its particle size was calculated. All experiments were performed in a triplicate manner, and their corresponding standard deviation was computed<sup>[17]</sup>.

#### **Friability:**

The mechanical robustness of the pellets was evaluated through a friability test, where lower friability scores denote enhanced mechanical integrity. It was assessed using a granule friability tester, and the results were expressed as the % weight loss after operating the apparatus at 200rpm for 4 min. (EF 1W, Electrolab India Pvt. Ltd, Mumbai, India)<sup>[18]</sup>.

#### **Pellet sphericity:**

The pellet's sphericity is denoted by the aspect ratio, which denotes the shape of the pellets. It was assessed by measuring the Feret diameter and its corresponding perpendicular diameter using a vernier caliper. These values were put into Equation 2 and calculate the aspect ratio<sup>[19]</sup>.

Aspect ratio=(Longest ferret diameter)/(Longest perpendicular diameter)×100 (2)

#### **In vitro buoyancy assessment:**

The buoyancy behaviour of both uncoated and coated LSH-GRFP was examined using the USP dissolution apparatus II in 900 ml of 0.1N HCl at 37°±0.5°.

The study comprised a 500 mg pellet sample that was gently dispersed on the surface of dissolution media and agitated using a paddle rotating at 50 rpm (4). After the designated agitation period, the number of pellets that remained floating on the surface of the dissolution media was recorded. The onset of buoyancy and total floating duration were determined by visual observation. The percentage of floating pellets was then calculated using the formula noted in Equation 3<sup>[20]</sup>.

% Floating pellets=(Number of floating pellets at measuring time)/(Initial number of pellets)×100 (3)

#### **Drug interaction by Fourier Transform Infrared Spectroscopy (FTIR):**

The potential interaction between LSH and excipients was characterised by comparing the FTIR spectrum of uncoated LSH-GRFP with pure LSH. The pure LSH and LSH-GRFP samples were first dried in a hot air oven (BTI-21, Bio-Techniques, India) to remove residual moisture. Each dried sample was then blended with potassium bromide and compressed into a pellet for spectral analysis. The obtained spectra were recorded using IR affinity-1 (Shimadzu Corporation, Kyoto, Japan)<sup>[21]</sup>.

#### **Phase transition assessment by Differential Scanning Calorimetry (DSC):**

The DSC thermogram offers critical insights into a range of characteristics, such as melting points, phase transitions, compatibility, and stability, which are crucial for the development of novel dosage forms. As a result, all these samples, including pure LSH and optimized uncoated LSH gastro-retentive floating pellets, underwent characterization through the DSC technique. In order to accomplish this, 5 mg of each sample was accurately weighed and sealed in an aluminum pan. The temperature of the sealed sample was allowed to equilibrate at 25°, followed by subjected to heating at temperatures ranging from 50° to 300°, with a consistent heating rate of 10°/min. During the analysis, dry nitrogen gas was utilized with a DSC-1821e instrument from Mettler Toledo AG, Analytical, Switzerland<sup>[22]</sup>.

#### **Surface morphology assessment:**

The surface morphological characteristics of uncoated and coated LSH-GRFP were examined using Scanning Electron Microscopy (SEM) on a JEOL JSM-7610F (Tokyo, Japan). The study included

characterization of surface texture, morphology, and pellet shape. The study comprised the dispersion of a small sample in deionised water and mounting it on a standard carbon-coated copper grid. The specimens were then observed under vacuum conditions with 200 kV accelerating voltage<sup>[23,24]</sup>.

### ***In vitro* drug release study:**

The drug release profile of LSH from uncoated and coated LSH GRFP was examined using the USP Type II dissolution apparatus of the Electro lab dissolution tester, having model TDT-08L. The study was performed in 900 ml of 0.5N HCl at  $37^{\circ}\pm 0.5^{\circ}$  with paddle rotation speed of 50 rpm. An equivalent amount of 40 mg of LSH, containing uncoated and

coated LSH pellets, was accurately weighed and introduced into the dissolution vessel. During the experimentation, 5 ml samples were withdrawn at predetermined time intervals as represented in fig. 1. The sink condition in the vessel was maintained by immediately replenishing an equal amount of fresh dissolution medium throughout the study<sup>[25]</sup>.

The withdrawal aliquot samples were filtered through Whatman grade 42 filter paper and analysed at 227 nm wavelength using a Shimadzu UV-visible spectrophotometer of model number UV-1800 (Japan). The comprehensive release kinetics underlying its mechanism of LSH from both pellets were fitted to different kinetic models<sup>[26]</sup>, and the data were summarised in Table 3.

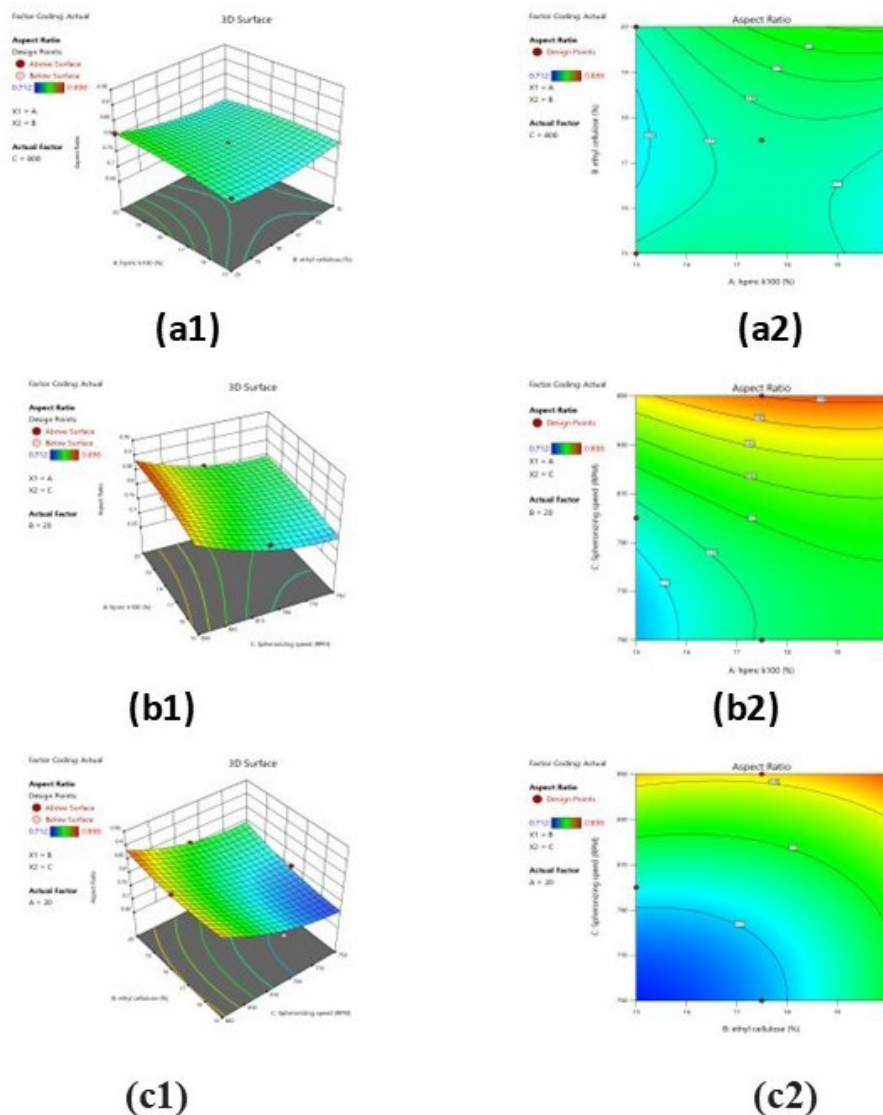


**Fig. 1:** 3D response graph and contour plot for aspect ratio are depicted in (a and b): For the interaction between HPMC concentration and ethyl cellulose at a constant spray drying speed; interaction between HPMC concentration and spray drying speed at a constant ethyl cellulose concentration and (c): For the interaction between ethyl cellulose concentration and spray drying speed at a constant HPMC concentration

**TABLE 3: STATISTICAL PARAMETERS FOR CONFIRMING THE QUADRATIC MATHEMATICAL MODEL FOR THE FOLLOWING RESPONSES**

Dependent variable/ Responses	SD	% C.V	R <sup>2</sup>	Adjusted R <sup>2</sup>	Predicted R <sup>2</sup>
Aspect ratio (Y <sub>1</sub> )	0.0207	2.6	0.9685	0.8741	0.8867
Total floating time (Y <sub>2</sub> )	0.2776	2.76	0.9876	0.9305	0.9353
Drug release (Y <sub>3</sub> )	0.7042	1.4186	0.9926	0.9106	0.9716

**Pharmacokinetic study:**

The study evaluated the comparative *in vivo* bioavailability and pharmacokinetic parameters of pure LSH, as well as optimized uncoated and coated LSH-GRFP, using 24 male Sprague-Dawley rats. The Sprague-Dawley male rats were approved by the IAEC of Dadasaheb Balpande College of Pharmacy under the approval number DBCOP/IAEC/1426/21-22/P10. The total weight of the rats was 200±50 g, and they adhered to all animal ethics guidelines. The experimental rats were maintained at a temperature of 22°±2° and provided a standard diet with water before drug treatment. Nonetheless, they abstained from food overnight before the experiment<sup>[27]</sup>. All rats were systematically allocated into four separate groups (I, II, III, and IV, n=6). The initial group serves as a control and is administered water exclusively. The II, III, and IV groups received treatment with dispersion of pure LSH, uncoated and coated LSH pellets in water with a dose equivalent to 10mg/kg orally in a fasted state, respectively<sup>[28]</sup>.

At a specific time interval, as depicted in fig. 1, the blood samples were withdrawn from the retro-orbital plexus and centrifuged using a REMI Model CM 12 Plus centrifuge for 10 min at 12 000 rpm at 4°. The plasma samples were decanted and subjected to single-step protein precipitation. Further, it was mixed with 0.2 ml quinine sulfate (0.5 g/ml in acetonitrile) as an internal standard. The samples were vortexed for 2 min and again centrifuged at 12 000 rpm for 10 min at 4°C. The resultant supernatant was collected and stored at -20° until further analysis. The plasma concentration of LSH was quantified using a Shimadzu Corporation spectrophotometer (Japan) with excitation wavelength 345 nm and emission wavelength 400 nm. The quantification was performed using a previously established calibration curve, and pharmacokinetic parameters were calculated using PK solver software<sup>[29]</sup>.

***In vivo* buoyancy study:**

For the *in vivo* buoyancy assessment, X-ray imaging techniques were utilized, specifically employing the Heliophos D system from Siemens. In preparation for this study, rats were fasted overnight. The coated LSH-GRFP, equivalent to 10mg/ml was orally administered to these rats *via* oral gavage. Followed by X-ray examinations were conducted at intervals of 6 h and 12 h. The duration for which the pellets remained buoyant within the stomach was determined through visual inspection<sup>[30]</sup>.

**RESULTS AND DISCUSSION**

The efficacy of extended-release LSH-GRFP is fundamentally rooted in its buoyancy properties. The HPMC exhibits hydrophilic properties, leading to its ability to hydrate and swell, ultimately resulting in the formation of a gel. Consequently, ethyl cellulose establishes a matrix-like configuration that regulates the release of the drug *via* mechanisms of diffusion and erosion. Nevertheless, this gel and matrix configuration lacks the capacity to produce Carbon Dioxide (CO<sub>2</sub>), which is essential for facilitating and sustaining buoyancy. Consequently, the incorporation of sodium bicarbonate is essential to produce the gas and establish a low-density system. The polymer PVP K 30 was incorporated to endure the pressure of the generated gas and prevent rupture. In addition to this, MCC imparts the necessary rheological characteristics and functions as a binding agent to secure the drug and excipients together. It facilitates the creation of a moist aggregate suitable for extrusion, resulting in robust and spherical pellets<sup>[31]</sup>.

The pelletization process was first optimized by adjusting three variables at three levels: the concentration of HPMC (X1), the concentration of ethyl cellulose (X2), and the spheronization speed (X3). Thirteen batches were developed in accordance with a Box-Behnken response surface model and

assessed for the quality fit of the model utilizing Design-Expert software, version 13. Multiple linear regression analysis was performed to develop polynomial equations, which incorporate interactions among variables. The most suitable mathematical models for the aspect ratio (Y1), total floating time (Y2), and cumulative % drug release (Y3) were identified as quadratic, as detailed in Equations 4, 5, and 6, respectively. The derived second-order regression equation indicated that all responses were influenced by all three variables during spononization. The positive values in all the equations indicated the collaborative effect of variables on responses<sup>[32]</sup>.

The selection of the quadratic model was based on a comprehensive evaluation of the experimental data. It involved the comparison of statistical indicators such as coefficient of variation (% CV), standard deviation, multiple correlation coefficient (R2), adjusted and predicted R2 were summarized in Table 3. The relationship between the formulation factors and measured responses was observed using three-dimensional response surface plots and corresponding contour plots, generated by varying two factors while keeping the third factor constant<sup>[33]</sup>.

$$Y1=97.63X1+2.73X2+0.5550X3+0.1125X12+0.02$$

$$50X23+0.1025X23+0.6250X12+0.6526X22+0.5350X32 \quad (4)$$

$$Y2=1.0137X1+1.32X2+0.4050X3+0.1050X12+0.125X13+0.0175X23+0.8300X12+0.1050X22+0.775X32 \quad (5)$$

$$Y3=0.072X1+0.0121X2+0.00639X3+0.0128X12+0.0053X13+0.0145X23+0.0145X12+0.0155X22+0.285X32 \quad (6)$$

The aspect ratio determines the sphericity of pellets, which in turn determines the uniformity of their surface. Fig. 2 and Equation 4 predict that HPMC, ethylcellulose, and spononizing speed all influence the sphericity of pellets. Both ethyl cellulose and HPMC form smoother and uniform film that reduces overall irregularity, leading to spherical pellets. From that, HPMC tends to produce the pellets with a higher aspect ratio compared to ethyl cellulose because HPMC forms a more flexible and cohesive film during spononization and gives greater elongation and less breakage during drying and handling. High spononization speed generally lowers the aspect ratio because spononization speed generates centrifugal and frictional forces. These forces break down the extrudate and colloid, frequently resulting decrease in aspect ratio<sup>[34]</sup>.

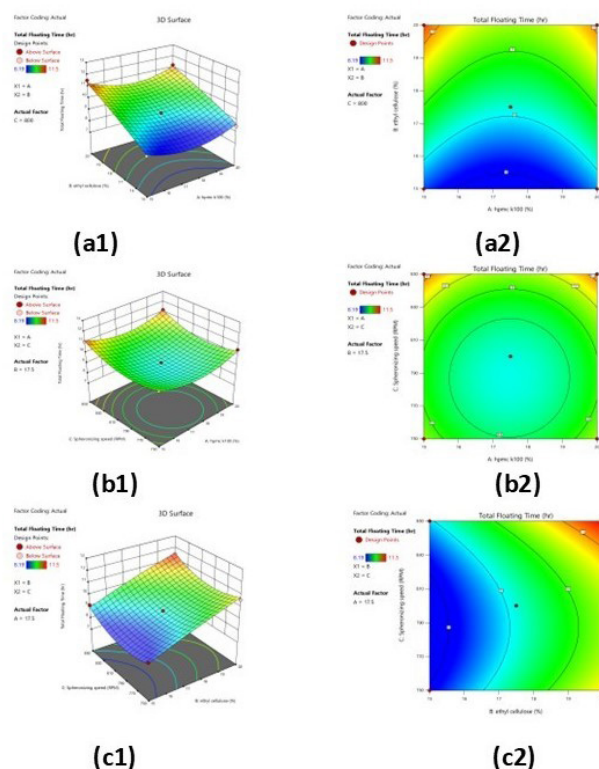
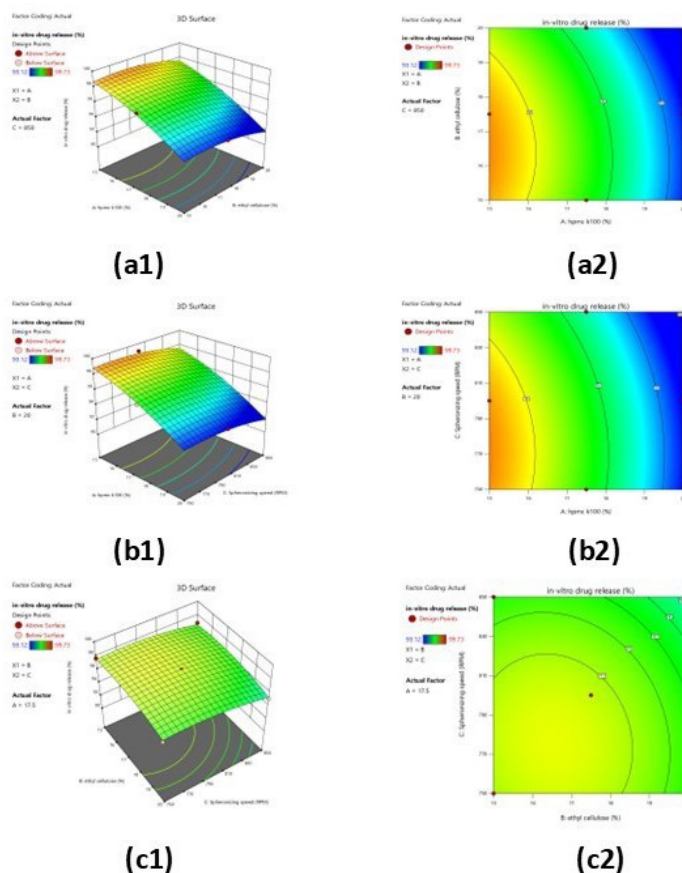


Fig. 2: 3D response graph and contour plot for floating time are depicted in (a and b): For the interaction between HPMC concentration and ethyl cellulose at a constant atomization speed; interaction between HPMC concentration and atomization speed at a constant ethyl cellulose concentration and (c): For the interaction between ethyl cellulose concentration and atomization speed at a constant HPMC concentration

Total floating time of the developed LSH pellets batches was observed in the range of  $8.19 \pm 0.05$  to  $11.42 \pm 0.12$  h. High floating time is beneficial for gastro retentive, which supports extended release and absorption of LSH in the upper part of the GIT. The 3D model plot and contour plot for total floating time are represented in fig. 3. At constant sponisation speed, the concentration of ethyl cellulose and HPMC gives positive effects on total floating time.

HPMC is a hydrophilic polymer that enhances hydration and swelling, which leads to faster

buoyancy and shorter floating lag time. However, Ethyl cellulose is a hydrophobic polymer, forming a barrier that delays water penetration and enhances the total floating time (34). Consequently, optimizing both concentrations improves the overall floating duration and the floating characteristics of the pellets. Furthermore, the speed of sponisation demonstrated a marginally beneficial impact on the floating behavior of the pellets. The sponising speed directly affects the shape, size, and density of pellets, which influence the buoyancy and improve the ability to float<sup>[35]</sup>.



**Fig. 3:** 3D response graph and contour plot for cumulative percentage drug release were shown in (a): The interaction between ethyl cellulose and HPMC concentration at a constant sponising speed value and (b): The interaction between HPMC concentration and sponising speed at a constant ethyl cellulose concentration and (c): The interaction between ethyl cellulose concentration and sponising speed at a constant HPMC concentration

The *in vitro* percentage of drug release ranged from  $91.28 \pm 2.23$  to  $97.69 \pm 2.35$  %. The maximum drug release observed in 0.1 N HCl at 12 h validated the sustained release and solubility of LSH in the upper gastrointestinal tract. It additionally facilitates the improvement of the oral bioavailability of LSH. Both polymers demonstrated a beneficial impact on the extended release of the drug. HPMC serves as a matrix former and quickly develops a viscous

or gel layer through the hydration of the polymeric surface upon contact with an aqueous liquid<sup>[36]</sup>. This layer acts as a physical barrier to access the water inside the pellets and the release of the drug through diffusion. Ethyl cellulose also controls the diffusion of the drug by forming a polymeric coating. It acts as a barrier and slows down the drug release, often combined with HPMC. Though sponisation speed cannot directly affect the drug release but it changes

the shape of pellets, which affects the drug release time and rate<sup>[37]</sup>.

From all thirteen batches, the highest response concerning all variables was found at batch FP7. Therefore, an overlay plot with a constriction of the margin near batch FP7 was designed and observe the yellow portion as the optimized region, as shown in fig. 4. From the overlay plot, batch B0 was developed as a checkpoint batch comprised of 19.25 % concentration of HPMC k100, 18.60 % concentration of ethyl cellulose, and 850 rpm of spheronizing speed. The % error in the predicted responses and the actual response of batch B0 was shown in Table 4, and the % error was found to be <5 % for all the responses and considered as an optimised batch.

Further, batch B0 was coated with ethyl cellulose and assessed for all physicochemical parameters as stated in Table 5. The sphericity of coated LSH pellets was increased by  $0.83\pm 0.08$ , which confirmed the uniform and smooth surface. The total floating time was also increased up to  $12.43\pm 0.10$ , which increased the residence time of pellets in the upper GIT and supports extended drug release of up to  $95.01\pm 1.34$  in 18 h.

The physicochemical parameters of all 13 batches predicted by Box Behnken design, optimised batch, and ethyl cellulose-coated LSH-GRFP batch were evaluated, including micromeritic properties, friability, hardness, drug content, and % flowing pellets, and represented in Table 6.

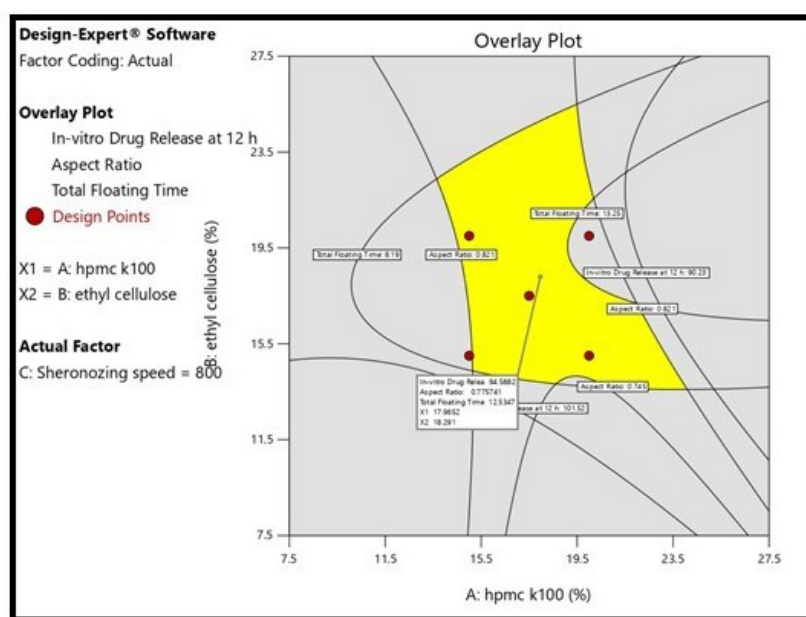


Fig. 4: The overlay plot for all three responses with the optimised region (yellow color) and checkpoint batch B0 with predicted responses

**TABLE 4: PREPARED BATCHES ACCORDING TO A BOX-BEHNKEN RESPONSE SURFACE MODEL WITH THREE INDEPENDENT VARIABLES AT THREE LEVELS**

Batch no.	Independent variable			Dependent variable		
	X <sub>1</sub> : HPMC K100 (%)	X <sub>2</sub> : Ethyl cellulose (%)	X <sub>3</sub> : Spheronizing speed (RPM)	Y <sub>1</sub> : Aspect ratio	Y <sub>2</sub> : Floating time (h)	Y <sub>3</sub> : <i>In vitro</i> drug release (%)
FP1	15	15	800	0.77±0.13	8.34±0.09	93.48±2.31
FP2	20	15	800	0.74±0.09	8.46±0.11	94.02±2.42
FP3	15	20	800	0.78±0.15	11.05±0.08	96.03±3.11
FP4	20	20	800	0.81±0.11	11.02±0.08	91.12±1.31
FP5	15	17.5	750	0.71±0.07	10.31±0.10	92.73±2.09

FP6	20	17.5	750	0.75±0.12	10.48±0.13	94.53±1.82
FP7	15	17.5	850	0.84±0.09	11.06±0.07	96.58±1.53
FP8	20	17.5	850	0.86±0.14	11.18±0.08	91.28±2.23
FP9	17.5	15	750	0.73±0.13	8.19±0.05	96.68±1.72
FP10	17.5	20	750	0.76±0.11	10.56±0.09	96.34±2.44
FP11	17.5	15	850	0.89±0.15	9.12±0.14	96.87±1.27
FP12	17.5	20	850	0.87±0.17	11.42±0.12	95.12±2.18
FP13	17.5	17.5	800	0.77±0.03	9.15±0.07	97.69±2.35

Note: All values are expressed as mean±standard deviation (n=3)

**TABLE 5: THE PREDICTED VALUE, ACTUAL VALUE, AND % ERROR IN ALL RESPONSES OF THE OPTIMISED BATCH (B0)**

Evaluation parameters	Batch B0		
	Predicted value	Actual value	% Error
Y <sub>1</sub> : Aspect ratio	0.777	0.81±0.10	3.28
Y <sub>2</sub> : Total floating time (h)	12.24	11.53±0.08	2.88
Y <sub>3</sub> : <i>In vitro</i> drug release (%)	95.09	96.74±1.34	3.38

Note: All values are expressed as mean ± standard deviation (n=3)

**TABLE 6: PHYSICO-CHEMICAL PARAMETERS EVALUATION OF ALL BATCHES**

Batch no.	Micromeritics Properties	% Drug content	% Floating pellets	Hardness kg/cm <sup>2</sup>	% Friability	dfs <sub>f</sub>	dfs <sub>f</sub>	dfs <sub>f</sub>
	Particle size distribution microns(μm)	Angle of repose (o)	Carr's index (%)	Hausner's ratio				
B0 (Optimized batch)	800-1000	28.18±1.69	14.64±0.94	1.05±0.02	96.31±2.52	91.28±1.02	1.96±0.13	0.31±0.01
Coated LSH-GRFP	800-900	27.04±1.16	14.23±1.23	1.08±0.06	96.26±2.51	95.32±1.17	2.07±0.09	0.21±0.02
FP1	850-1000	29.16±2.06	16.51±0.73	1.32±0.15	97.24±3.74	91.65±1.94	1.72±0.12	0.35±0.02
FP2	1000-1200	30.27±1.89	17.82±1.03	1.42±0.07	97.32±2.92	89.76±1.38	2.04±0.06	0.11±0.01
FP3	800-1000	29.14±1.17	17.26±0.78	1.37±0.06	93.2± 1.76	92.37±2.03	1.38±0.17	0.32±0.02
FP4	850-1000	34.08±2.18	18.75±2.12	1.15±0.14	91.75±1.09	91.71±1.46	1.62±0.07	0.56±0.03
FP5	900-1200	29.15±1.14	17.62±1.52	1.38±0.13	92.12±1.54	87.08±2.25	1.74±0.26	0.12±0.01
FP6	1000-1200	30.53±1.09	18.43±0.95	1.24±0.09	97.31±2.64	92.62±2.71	1.27±0.09	0.14±0.01

FP7	850-1000	27.48±1.16	14.37±1.07	1.26±0.12	96.69±1.82	92.47±2.48	1.84±0.16	0.36±0.02
FP8	850-1000	31.37±2.18	18.32±2.15	1.31±0.07	91.47±1.24	89.27±2.63	1.52±0.06	0.32±0.01
FP9	850-1000	28.52±1.05	17.79±2.03	1.51±0.11	93.23±1.19	92.71±1.65	1.81±0.17	0.45±0.03
FP10	1000-1200	32.38±1.26	19.82±0.92	1.43±0.06	94.30±1.37	89.63±1.24	1.75±0.19	0.52±0.02
FP11	900-1100	28.22±1.03	17.28±1.47	1.14±0.08	93.09±1.09	90.47±2.41	2.02±0.25	0.13±0.01
FP12	1000-1200	32.72±2.72	19.39±1.81	1.23±0.15	96.42±2.67	88.62±1.53	1.68±0.16	0.33±0.01
FP13	1000-1200	31.35±1.92	19.91±1.58	1.58±0.32	93.62±1.83	91.72±1.29	1.53±0.23	0.43±0.02

**Note:** All values are expressed as mean±standard deviation (n=3)

The drug content was assessed using UV-spectroscopy, revealing a range of 91.47±1.24 to 97.32±2.92. The results indicated that all pellet batches demonstrated commendable consistency in drug content. The optimized batch of LSH GRFP (B0) exhibited a drug content of 96.31±2.52 %. Analysis of the flow properties across all batches, as indicated by the angle of repose, Carr's consolidation index, and Hausner's ratio, confirmed that each batch exhibited favorable flow characteristics. The angle of repose for optimized batch B0 was determined to be 28.18±1.69, while Carr's consolidation index measured 14.64±0.94, and Hausner's ratio was calculated at 1.05±0.02. The optimized batch (B0) exhibited a hardness of 1.96±0.13 kg/cm and a friability of 0.31±0.01 %, demonstrating its robust resistance to mechanical stress during the coating process. The data regarding particle size distribution indicated that the sizes of all 13 batches fell within the range of 800-1200 µm, with the optimized B0 batch specifically measuring between 800-1000 µm, thereby affirming its narrow size distribution.

After coating with ethyl cellulose, it was found that the micromeritics properties of the LSH-GRFP were enhanced, as shown in Table 6, exhibiting excellent flow. The % floating pellets were significantly enhanced after coating due to the hydrophobic nature of ethyl cellulose hindering water penetration and increasing the time and % of floated pellets<sup>[38]</sup>.

The surface morphological characteristics of uncoated and coated LSH-GRFP were assessed by SEM. The image revealed from uncoated LSH-GRFP was predominantly spherical geometry with a mildly textured surface. In comparison, the coated LSH-GRFP displayed a noticeably smoother and more uniform surface topography, confirming the formation of a consistent ethyl cellulose coating as

shown in fig. 5.

The FTIR spectrum of pure LSH displayed distinct characteristic absorption bands, including an N-H stretching vibration at 3431 cm<sup>-1</sup>, an aromatic C=C stretching band at 1564 cm<sup>-1</sup>, and a C-Cl stretching peak at 777 cm<sup>-1</sup>. Additional prominent signals corresponding to the C-N stretch and C-H stretch were observed at 1186 cm<sup>-1</sup> and 2914 cm<sup>-1</sup>, respectively (fig. 6a). In the uncoated LSH-GRFP formulation, LSH did not interact with HPMC and ethyl cellulose. The HPMC and ethyl cellulose polymers form a matrix structure in pellet formulation, and LSH was physically entrapped within it, which supports the extended release. As the FTIR spectra of LSH-GRFP were quite different, they showed shifting of the peaks with a change in bond strength and length. The characteristic stretching bands associated with N-H stretch and aromatic C=C stretch slightly shift at 3747 cm<sup>-1</sup> and at 1541 cm<sup>-1</sup>. Other characteristic stretching bands of LSH merge with the functional group of ethyl cellulose and HPMC and form a broad peak, as shown in fig. 6b.

The pronounced endothermic peak observed at 269°, characterized by a significant energy value of -146.43 Joule/gram, is indicative of the melting point and crystalline structure of pure LSH, as illustrated in fig. 7a. The DSC thermogram of LSH pellets revealed a shift in the endothermic peak at 147°, accompanied by a decrease in energy to -74.36 J/g. The thermal behavior and potential changes in crystalline LSH were characterised by comparing DSC thermograms of pure LSH with uncoated LSH-GRFP. The thermogram depicted the heat flow as a function of thermal transition and the overall stability of the drug. Pure LSH exhibited a sharp endothermic peak at 269° with an enthalpy value of -146.43 J/g, corresponding to its melting point and confirming its

crystalline nature as depicted in fig. 7a. In contrast, the DSC profile of formulated pellets demonstrated a shifted endothermic broad peak at 147° with a reduced enthalpy of -74.36 J/g, indicating a phase

transition in formulation as illustrated in fig. 7b. This observation indicates the entrapment of LSH within the matrix structure formed by HPMC and ethyl cellulose in the pellets.

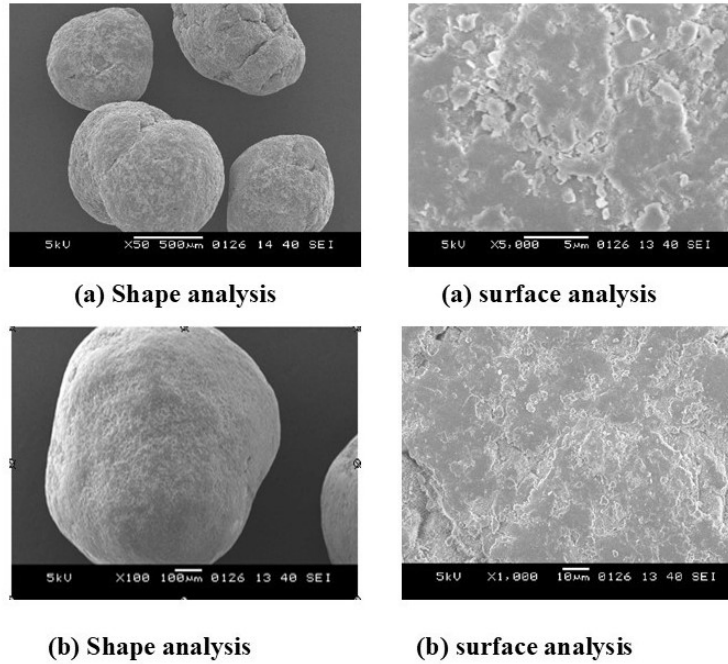
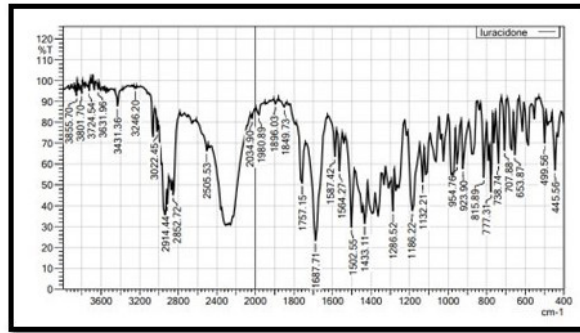
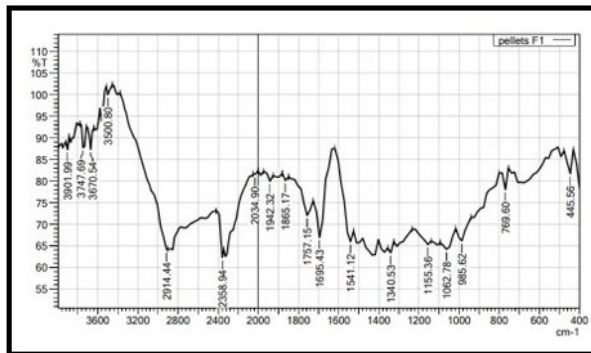


Fig. 5: SEM picture of (a): Uncoated LSH GRFP and (b): Coated LSH GRFP, demonstrating their spherical shape and smooth surface morphology

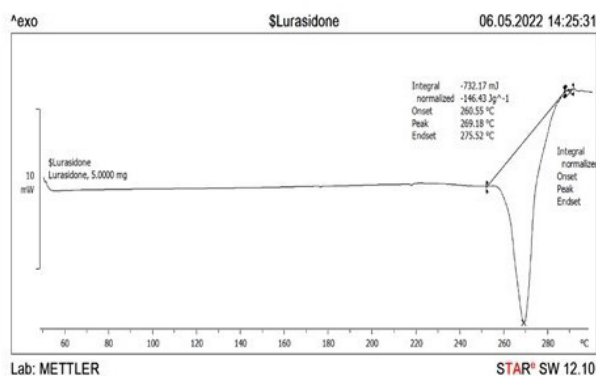


(a)

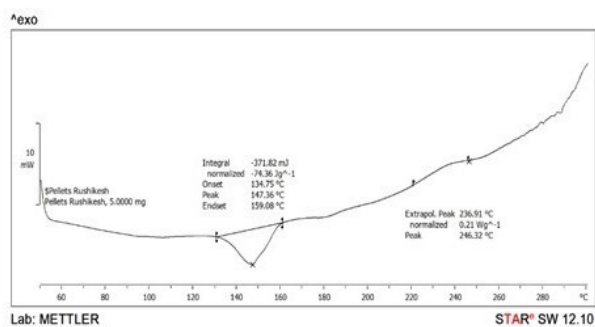


(b)

Fig. 6: FTIR spectra for (a): Pure LSH and (b): Uncoated LSH GRFP, suggesting successful embedding of LSH in HPMC and ethyl cellulose-comprised floating pellets



(a)



(b)

Fig. 7: The DSC thermogram for (a): Pure LSH and (b): Uncoated LSH-GRFP validates the thermal transition and thermal stability of LSH within the gastro retentive floating pellets composed of HPMC and ethyl cellulose

The cumulative % LSH release from all batches was conducted *in vitro* at pH 4.5, as illustrated in Table 7. The B0 batch was optimized according to all responses concerning % aspect ratio, % floating pellets, and *in vitro* drug release. Further, it was coated with 5 % w/v ethyl cellulose in isopropyl alcohol. The cumulative % drug release profile of pure LSH, batch B0, and ethyl cellulose-coated LSH-GRFP over time is represented in fig. 8. The low solubility of pure LSH showed  $19.23 \pm 1.02$  % release in 12 h. However, the release profile of LSH from uncoated pellets

followed a burst release of  $15.03 \pm 1.31$  % in the initial 3 h, then followed by extended release up to 12 h that reaching  $96.74 \pm 1.34$ . The initial burst release was achieved as a result of the free drug present on the surface; further, it followed diffusion and erosion. The HPMC in the pellets can hydrate, swell, and leach out the drug from pores and channels that facilitate drug release. In addition, ethyl cellulose primarily controlled the drug release by diffusion or formation of osmotic pressure through the polymeric membrane or matrix structure<sup>[39,40]</sup>.

TABLE 7: THE REGRESSION COEFFICIENT AND RELEASE EXPONENT OF LSH FROM DEVELOPED FLOATING PELLETS, SUGGESTING A DRUG RELEASE KINETIC MODEL

Sr. no.	Formulation	R2 (coefficient of determination)				Release exponent
		Zero order	First order	Higuch	Hixon Crowell cube root	
1	Pure LSH	0.8132	0.8521	0.9367	0.8291	0.6172
2	Uncoated LSH-GRFP	0.7831	0.8251	0.9873	0.7841	0.5162
3	Coated LSH-GRFP	0.8032	0.9152	0.9734	0.8329	2.1042

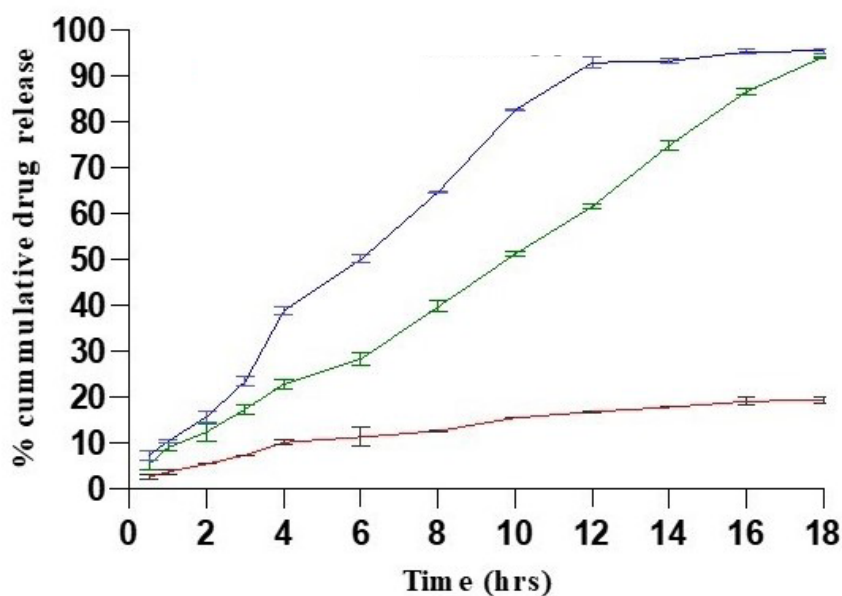


Fig. 8: TCumulative % LSH release from pure LSH, uncoated LSH-GRFP, and coated LSH-GRFP. All values are represented as mean $\pm$ SEM (n=3)

Note: (—): Uncoated LSH floating pellets; (—): Coated LSH floating pellets and (—): Pure LSH

The LSH release from uncoated and coated LSH-GRFP fit into a different kinetic model, and observed that it followed the Higuchi model. It described drug release through the matrix by a diffusion process and followed Fick's law of diffusion, which is square root of time dependent, with  $r^2$  value of 0.9905.

After coating of LSH pellets with ethyl cellulose, the release profile followed sustained release up to 18 h that reaching  $95.01 \pm 1.34$ , and also followed the Higuchi model for release kinetics. It was suggested that the coating of ethyl cellulose controlled the diffusion and remained intact during the release process. The hydrophobic surface of ethyl cellulose releases the drug by eroding the surface. After erosion, the matrix structure of HPMC supports the drug release<sup>[41]</sup>. The release exponent ( $n$ ) of both uncoated and coated LSH GRFP was 0.49 and 0.62, respectively, as shown in Table 7, which suggests that drug release followed anomalous transport. It was suggested that the porous matrix structure of HPMC and ethyl cellulose supported the release of LSH. The drug spreading coefficient in this mechanism remains constant, and the drug release is consistently influenced by sink conditions.

In pharmacokinetic assessment, a single oral dose equivalent to 10 mg of pure LSH, uncoated and coated LSH-GRFP dispersion, was orally administered to Sprague-Dawley rats. The plasma LSH concentrations

were quantified, and the pharmacokinetic parameters were determined. The relative bioavailability of uncoated and coated LSH-GRFP was estimated by assessing total AUC as compared to pure LSH by non-compartmental analysis. Subsequently, half-life, clearance, and other pharmacokinetic parameters were also determined and stated in Table 8. The observed result showed that the enhanced solubility and absorption of uncoated and coated LSH-GRFP significantly increased relative bioavailability compared to pure LSH. The optimised concentration of HPMC and ethyl cellulose enhanced the total buoyancy of LSH pellets, which supports increasing its retention time in the upper GIT, which helps to increase the absorption of LSH and ultimately increases the relative bioavailability compared to pure LSH<sup>[42]</sup>, as represented in Table 8 and fig. 9. The  $C_{max}$  and AUC of pure LSH in plasma were found to be  $220.71 \pm 12.82$  ng/ml and  $1095.75 \pm 52.75$  ng/ml\*h, respectively. The AUC of uncoated and coated LSH pellets was increased up to fivefold and sevenfold, respectively.

In coated LSH-GRFP, the hydrophobic coating of ethyl cellulose controls the release rate of LSH. It forms a barrier that prevents water penetration and displaces air within the matrix structure of pellets. Therefore, it enhances floating time and improves the dissolution of LSH in the upper GIT<sup>[43]</sup>. The value of  $T_{max}$  and MRT of coated LSH pellets was

found to be 4 h and  $23.05 \pm 0.18$  h, respectively, which was nearly double compared to uncoated LSH pellets. Therefore, it was suggested that coated LSH gastro retentive floating pellets would increase the oral bioavailability and therapeutic efficacy of LSH.

The *in vivo* buoyancy study using X-ray scanning was carried out to track the location and behaviour of coated LSH gastro retentive floating pellets in the upper GIT of Sprague-Dawley rats. This is an important parameter to determine the floating time

of pellets in the stomach. After oral administration of coated LSH gastro retentive floating pellets dispersion, X-ray scanning was taken for 6 and 12 h. It was observed that coated LSH pellets floated in the stomach up to 12 h, as shown in fig. 10. The HPMC and ethyl cellulose matrix structure was designed to float the pellets. In addition, the hydrophobic surface of the ethyl cellulose coating forms a barrier that prevents water penetration and displaces air within the matrix structure of pellets, which also helps to increase the buoyancy property of pellets<sup>[44]</sup>.

**TABLE 8: PHARMACOKINETIC PARAMETERS OF LSH AFTER ORAL ADMINISTRATION OF PURE LSH, UNCOATED LSH-GRFP, AND COATED LSH GRFP DISPERSION**

Sr. no.	Parameters	Pure LSH	Uncoated LSH -GRFP	Coated LSH-GRFP
1	$T_{max}$ (h)	2	3	4
2	$C_{max}$ (ng/ml)	$220.71 \pm 12.82$	$618.72 \pm 21.96$	$669.73 \pm 27.09$
3	$T_{1/2}$ (h)	$4.49 \pm 0.18$	$6.47 \pm 0.16$	$16.34 \pm 0.12$
4	MRT (h)	$6.29 \pm 0.15$	$10.57 \pm 0.12$	$23.05 \pm 0.18$
5	$AUC_{0-12h}$ (ng.h/ml)	$1095.75 \pm 52.75$	$5060.82 \pm 87.89$	$7867.30 \pm 62.86$

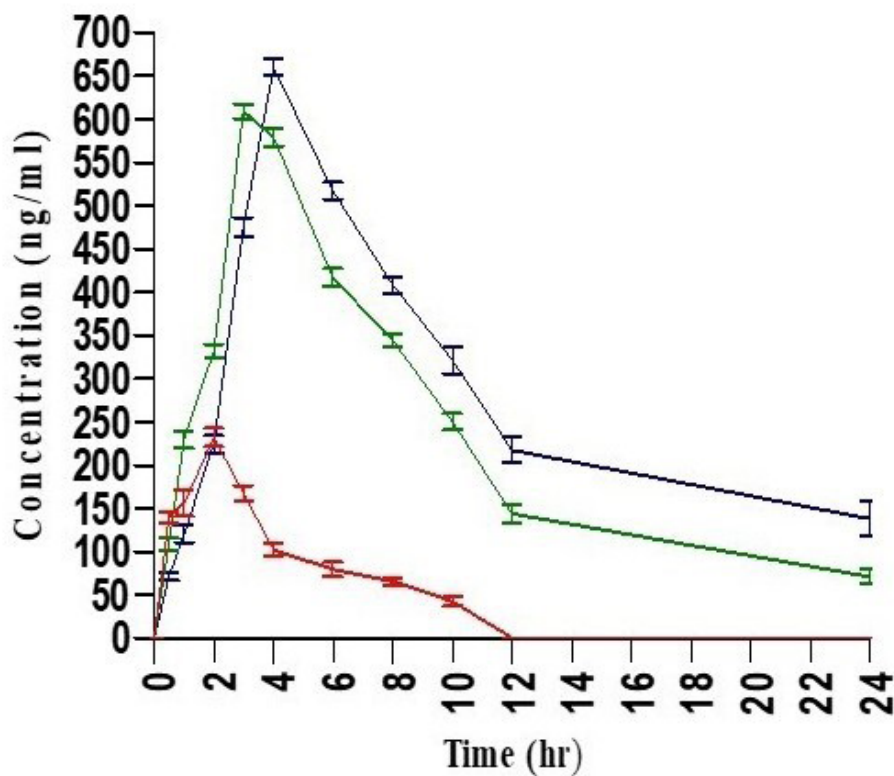


**Fig. 9: Plasma pharmacokinetics after oral administration of pure LSH, uncoated LSH-GRFP, and coated LSH-GRFP dispersion in water. All values are represented as mean $\pm$ SD (n=3)**

Note: ( — ): Pure LSH; ( — ): LSH gastroretentive floating pellets and ( — ): Coated LSH gastroretentive floating pellets



After 4 h



After 12 h

Fig. 10: X-ray scanning images of Sprague-Dawley rats after oral administration of coated LSH-GRFP dispersion after 4 h and 12 h confirmed its *in vivo* buoyancy

The present study examined the oral bioavailability and pharmacokinetics of gastro retentive floating pellets of LSH. For that, the gastro retentive floating pellets of LSH were developed by means of the extrusion-spheronization technique. It was optimized through 33 factorial Box-Behnken design by focusing on aspect ratio, total floating time, and *in vitro* drug release. The optimized batch B0 was further coated with ethyl cellulose to enhance gastric retention and floating time. The coated LSH pellets showed improved buoyancy up to 12 h with extended *in vitro* LSH release up to 18 h. This confirms that the developed coated LSH pellets act as a promising platform for gastric retention and offer an extended period of release. According to the pharmacokinetic parameter, the coated LSH pellets have  $23.05 \pm 0.18$  h MRT with  $C_{max}$  and relative bioavailability enhanced three to four-fold compared to pure LSH. It strongly supports the hypothesis that coated LSH gastro retentive floating pellets could remain in the abdomen for a long time to absorb the drug and enhance its oral bioavailability, instead of pure LSH.

### Conflict of interests:

The authors declared no conflict of interests.

### REFERENCES

- Sathisaran I, Dalvi SV. Engineering cocrystals of poorly water-soluble drugs to enhance dissolution in aqueous medium. *Pharmaceutics* 2018;10(3):108.
- Thakur A, Thipparaboina R, Kumar D, Gouthami KS, Shastri NR. Crystal engineered albendazole with improved dissolution and material attributes. *CrystEngComm* 2016;18(9):1489-94.
- Patil H, Tiwari RV, Repka MA. Hot-melt extrusion: From theory to application in pharmaceutical formulation. *Aaps PharmSciTech* 2016;17(1):20-42.
- Lunio R, Sawicki W, Skoczen P, Walentynowicz O, Kubasik-Juraniec J. Compressibility of gastroretentive pellets coated with Eudragit NE using a single-stroke and a rotary tablet press. *Pharm Dev Technol* 2008;13(4):323-31.
- Sheikh FA, Hussain MA, Ashraf MU, Haseeb MT, Farid-ul-Haq M. Linseed hydrogel based floating drug delivery system for fluoroquinolone antibiotics: Design, *in vitro* drug release and *in vivo* real-time floating detection. *Saudi Pharm J* 2020;28(5):538-49.
- Ramteke S, Haigune N, More S, Pise S, Pise A, Kharwade R. Flaxseed Mucilage Hydrogel based Floating Drug Delivery System: Design and Evaluation. *Res J PharmTechnol* 2022;15(4):1549-54.
- Franc A, Vetchý D, Fülöpová N. Commercially available enteric empty hard capsules, production technology and application. *Pharmaceutics* 2022;15(11):1398.
- Halling Folkmar Andersen A, Tolstrup M. The potential of long-acting, tissue-targeted synthetic nanotherapy for delivery of antiviral therapy against HIV infection. *Viruses* 2020;12(4):412.
- Kotta S, Aldawsari HM, Badr-Eldin SM, Nair AB, Kaleem M, Dalhat MH. Thermosensitive hydrogels loaded with resveratrol nanoemulsion: formulation optimization by central composite design and evaluation in MCF-7 human breast cancer cell lines. *Gels* 2022;8(7):450.
- Majeed SM, Al-Shaheen MK, Al-Zidan RN, Mahmood SM. Multiple Unite Pellet Systems (MUPS) as drug delivery model. *J Drug Deliv Ther* 2020;10(6):231-5.
- Magalhães J, Chaves L, Vieira A, Santos S, Pinheiro M, Reis S. Optimization of rifapentine-loaded lipid nanoparticles using a quality-by-design strategy. *Pharmaceutics* 2020;12(1):75.
- Kharwade R, Ali N, Gangane P, Pawar K, More S. Of tioconazole-loaded transferosomal hydrogel for the effective treatment of atopic dermatitis: *In vitro* and. *Gels* 2023;9(303):1-20.
- Zakowiecki D, Frankiewicz M, Hess T, Cal K, Gajda M, Dabrowska J, *et al.* Development of a biphasic-release multiple-unit pellet system with diclofenac sodium using novel calcium phosphate-based starter pellets. *Pharmaceutics* 2021;13(6):805.
- Ragnarsson G, Sandberg A, Jonsson UE, Sjögren J. Development of a new controlled release metoprolol product. *Drug Dev Industrial Pharm* 1987;13(9-11):1495-509.
- Bodmeier R. Tableting of coated pellets. *Eur J Pharm Biopharm* 1997;43(1):1-8.

16. Kharwade R, Mahajan N, Ali S, Chakolkar M, Jain S, More S. Development and characterization of genistein-loaded silver nanoparticles for the induction of apoptosis on human hepatocellular carcinoma cell lines. *Bionanoscience* 2025;15(2):227.
17. Gangane P, Yadav A, Kharwade R, More S, Salunkhe K, Dangre P. Fabrication of enteric coated mucoadhesive pellets of Tofacitinib citrate for treatment of ulcerative colitis. *Particulate Sci Technol* 2025;43(2):257-68.
18. RS K, SM M. Formulation and evaluation of gastroretentive floating tablet using Hibiscus rosa-sinensis mucilage. *Asian J Pharm Clin Res* 2017;10(3):444-8.
19. Podczeczek F, Rahman SR, Newton JM. Evaluation of a standardised procedure to assess the shape of pellets using image analysis. *Int J Pharm* 1999;192(2):123-38.
20. Gupta R, Pathak K. Optimization studies on floating multiparticulate gastroretentive drug delivery system of famotidine. *Drug Devel Industr Pharm* 2008;34(11):1201-8.
21. Kharwade R, Kazi M, Mahajan N, Badole P, More S, Kayali A, *et al.* Mannosylated PAMAM G2 dendrimers mediated rate programmed delivery of efavirenz target HIV viral latency at reservoirs. *Saudi Pharm J* 2024;32(10):102154.
22. More SM, Rashid MA, Kharwade RS, Taha M, Alhamhoom Y, Elhassan GO, *et al.* Development of solid self-nanoemulsifying drug delivery system of rhein to improve biopharmaceutical performance: Physicochemical characterization, and pharmacokinetic evaluation. *Int J Nanomed* 2025;20:267-91.
23. Win KY, Feng SS. Effects of particle size and surface coating on cellular uptake of polymeric nanoparticles for oral delivery of anticancer drugs. *Biomaterials* 2005;26(15):2713-22.
24. Ang BC, Yaacob II, Nurdin I. Investigation of Fe<sub>2</sub>O<sub>3</sub>/SiO<sub>2</sub> nanocomposite by FESEM and TEM. *J Nanomater* 2013;2013(1):980390.
25. Sun SB, Liu P, Shao FM, Miao QL. Formulation and evaluation of PLGA nanoparticles loaded capecitabine for prostate cancer. *Int J Clin Exp Med* 2015;8(10):19670.
26. Salve V, Mishra R, Nandgude T. Development and optimization of a floating multiparticulate drug delivery system for norfloxacin. *Turkish J Pharm Sci* 2019;16(3):326.
27. Katz RJ. Animal models and human depressive disorders. *Neurosci Biobehav Rev* 1981;5(2):231-46.
28. Kharwade R, More S, Suresh E, Warokar A, Mahajan N, Mahajan U. Improvement in bioavailability and pharmacokinetic characteristics of efavirenz with booster dose of ritonavir in PEGylated PAMAM G4 dendrimers. *AAPS PharmSciTech* 2022;23(6):177.
29. El-Say KM. Maximizing the encapsulation efficiency and the bioavailability of controlled-release cetirizine microspheres using Draper-Lin small composite design. *Drug Design Devel Ther* 2016:825-39.
30. Jagdale SC, Suryawanshi VM, Pandya SV, Kuchekar BS, Chabukswar AR. Development of press-coated, floating-pulsatile drug delivery of lisinopril. *Sci Pharm* 2014;82(2):423.
31. Pagariya TP, Patil SB. Development and optimization of multiparticulate drug delivery system of alfuzosin hydrochloride. *Colloids Surfaces B Biointerfaces* 2013;102:171-7.
32. Kharwade R, Mahajan N, More S, Warokar A, Mendhi S, Dhobley A, *et al.* Effect of PEGylation on drug uptake, biodistribution, and tissue toxicity of efavirenz-ritonavir loaded PAMAM G4 dendrimers. *Pharm Devel Technol* 2023;28(2):200-18. [Crossref] [Google Scholar] [PubMed]
33. Veerubhotla K, Walker RB. Application of quality by design principles for optimizing process variables of extrusion and spheronization of a captopril pellet formulation. *Indian J Pharm Sci* 2020;82(1):76-84.
34. Garg AK, Kumar A, Rani S, Singh M, Sharma A, Kumar R. Formulation and evaluation of chronotherapeutic pulsatile drug delivery system containing rabeprazole sodium. *J Appl Pharm Sci* 2017;7(2):093-100.
35. Nicklasson F, Alderborn G. Modulation of the tableting behaviour of microcrystalline cellulose pellets by the incorporation of polyethylene glycol. *Eur J Pharm Sci* 1999;9(1):57-65.
36. Natarajan V, Krithica N, Madhan B, Sehgal PK. Formulation and evaluation of quercetin polycaprolactone microspheres for the treatment of rheumatoid arthritis. *J Pharm Sci* 2011;100(1):195-205.
37. Bhattacharya S, Prajapati BG. Formulation, design and development of ciprofloxacin hydrochloride floating bioadhesive tablet. *E-J Sci Technol* 2017;12(3).
38. Pai R, Kohli K, Shrivastava B. Compression and evaluation of extended release matrix pellets prepared by the extrusion/spheronization process into disintegrating tablets. *Brazil J Pharm Sci* 2012;48(1):117-29.
39. Yuan Z, Gu X. Preparation, characterization, and *in vivo* study of rhein-loaded poly (lactic-co-glycolic acid) nanoparticles for oral delivery. *Drug Design Devel Ther* 2015:2301-9.
40. Fu Y, Kao WJ. Drug release kinetics and transport mechanisms of non-degradable and degradable polymeric delivery systems. *Expert Opin Drug Deliv* 2010;7(4):429-44.
41. Marin E, Briceño MI, Caballero-George C. Critical evaluation of biodegradable polymers used in nanodrugs. *Int J Nanomed* 2013:3071-91.
42. Parikh A, Kathawala K, Tan CC, Garg S, Zhou XF. Development of a novel oral delivery system of edaravone for enhancing bioavailability. *Int J Pharm* 2016;515(1-2):490-500.
43. Emad NA, Sultana Y, Aqil M, Saleh A, Nasr FA. Omega-3 fatty acid-based self-microemulsifying drug delivery system (SMEDDS) of pioglitazone: Optimization, *in vitro* and *in vivo* studies. *Saudi J Biolog Sci* 2023;30(9):103778.
44. Li Q, Huang W, Yang J, Wang J, Hu M, Mo J, *et al.* Gastric retention pellets of edaravone with enhanced oral bioavailability: Absorption mechanism, development, and *in vitro/in vivo* evaluation. *Eur J Pharm Sci* 2018;119:62-9.